

Transient response of 2D functionally graded beam structure

Mohamed A. Eltahaer^{*1,2} and Şeref D. Akbaş^{3a}

¹Mechanical Engineering Department, Faculty of Engineering, King Abdulaziz University, P.O. Box 80204, Jeddah, Saudi Arabia

²Department of Mechanical Design & Production, Faculty of Engineering, Zagazig University, P.O. Box 44519, Zagazig, Egypt

³Department of Civil Engineering, Bursa Technical University, Bursa, Turkey

(Received October 24, 2019, Revised February 12, 2020, Accepted February 21, 2020)

Abstract. The objective of this article is investigation of dynamic response of thick multilayer functionally graded (FG) beam under generalized dynamic forces. The plane stress problem is exploited to describe the constitutive equation of thick FG beam to get realistic and accurate response. Applied dynamic forces are assumed to be sinusoidal harmonic, sinusoidal pulse or triangle in time domain and point load. Equations of motion of deep FG beam are derived based on the Hamilton principle from kinematic relations and constitutive equations of plane stress problem. The numerical finite element procedure is adopted to discretize the space domain of structure and transform partial differential equations of motion to ordinary differential equations in time domain. Numerical time integration method is used to solve the system of equations in time domain and find the time responses. Numerical parametric studies are performed to illustrate effects of force type, graduation parameter, geometrical and stacking sequence of layers on the time response of deep multilayer FG beams.

Keywords: forced vibration; transient response; 2D deep beam; multilayered functionally graded; finite element; implicit time integration

1. Introduction

During last decades, functionally graded materials (FGM), which are advanced classes of composite materials whose composition designed to change continuously within the spatial dimensions of structures, have been used in many applications such as aerospace, nuclear science, optics, chemistry, biomedical, defense, automotive, energy conversion, micro/nano-electro-mechanical system (MEMS/NEMS) and atomic force microscopes (AFMs) Alshorbagy (2011) and Eltahaer *et al.* (2013).

Since FGMs are promising in numerous applications, more researchers have been investigated forced vibrations of FGM beam and plate structures in both macro-scale and nano-scale theories. He *et al.* (2001) developed a finite element formulation based on classical laminated plate theory for the vibration control of FGM plates with integrated piezoelectric sensors and actuators. Yang *et al.* (2008) presented an analytical solution of free and forced vibrations of inhomogeneous beams containing open edge cracks and subjected to an axial compressive force along the longitudinal direction. Xiang and Yang (2008) studied free and forced vibrations of sandwich FG beam of variable thickness under thermally induced initial stresses within the framework of Timoshenko beam theory. Şimşek and Kocatürk (2009) and Şimşek (2010) investigated free vibration characteristics and dynamic behaviors of FG

simply supported beams under a concentrated moving harmonic load. Doroushi *et al.* (2011) investigated free and forced vibration characteristics of an FG beam under thermo-electro-mechanical loads by using the higher-order shear deformation beam theory. Shooshtari and Rafiee (2011) presented multiple time scale solutions to study the nonlinear forced vibration of FG beam made including von Kármán geometric nonlinearity. Assie *et al.* (2011) developed an efficient numerical algorithm to investigate the dynamic transient response of orthotropic viscoelastic composite laminates under step-pulse and sin-pulse forces. Malekzadeh and Monajjemzadeh (2013, 2015) investigated linear and nonlinear dynamic responses FG plates in thermal environment under moving load includes the effects of initial thermal stresses and elastic foundations effects. Eltahaer *et al.* (2014) studied free vibration of nonlinear material graduations of nonlocal Timoshenko nanobeams by using finite element method.

Su *et al.* (2016) developed a unified solution for free and transient vibration response of FG piezoelectric curved beam within the framework of Timoshenko beam theory. Wang and Wu (2016) studied dynamic response of an axially FG beam under thermal environment and subjected to a moving harmonic load within frameworks of classical and Timoshenko beam theories. Akbaş (2016 & 2017) exploited modified couple stress theory to investigate the dynamic response of simple supported viscoelastic nanobeams rested on Winkler-Pasternak elastic foundation and excited by a transverse triangular impulse force. Akbaş (2018a&b) modified his previous model to include crack effect on the dynamic response of viscoelastic behaviors of nanobeams. Akbaş (2018c) investigated free and forced vibration of a bi-material composite beam. Albino *et al.* (2018) studied nonlinear dynamic behaviors of risers

*Corresponding author, Professor

E-mail: meltahaer@kau.edu.sa; mmeltahaer@zu.edu.eg

^a Professor

E-mail: serefda@yahoo.com; seref.akbas@btu.edu.tr

manufactured with functionally graded materials and modeled by 3D beam element. Andrianov *et al.* (2018) defined and solved the problem of an optimized structural topology of the simply supported beam made from functionally graded material (FGM) enabling achievement of a maximum buckling load. Eltahaer *et al.* (2018a) and Attia *et al.* (2018) analyzed thermoelastic crack pipe manufactured by FGM and conveyed natural gas by using finite element method. Chen *et al.* (2018) investigated thermo-elastic vibration behaviors of FGM beams with general boundary conditions by using a higher-order shear deformation beam theory. Eltahaer *et al.* (2018b) demonstrated an analytical solution of resonance frequencies of size dependent regular square perforated nonlocal nanobeams. Huang *et al.* (2018) illustrated the effect of material gradation through the axial direction on whirling frequencies and critical speeds of a spinning Timoshenko beam.

Akbaş (2019a) studied nonlinear behavior of a FG cantilever beam under non-uniform hygrothermal effect and exploited finite element method and Newton-Raphson method with incremental displacement to solve proposed model. Akbaş (2019b) analyzed forced vibration of sandwich deep beams made of sandwich FGM including porosity effects. Abdalrahmaan *et al.* (2019) and Almitani *et al.* (2019) developed a unified mathematical model to investigate free and forced vibration responses of perforated thin and thick beams. Eltahaer *et al.* (2019a) illustrated influences of sine and cosine periodic and nonperiodic imperfections modes on buckling, postbuckling and dynamics of beam rested on nonlinear elastic foundations. Eltahaer *et al.* (2019b) studied bending and vibrational behaviors of piezoelectric nonlocal nanobeam including surface elasticity by using finite element method. Esen (2019) developed a modified finite element model to analyze the transverse vibrations of Timoshenko FG beams rested on two-parameter foundations and subjected to a variable-velocity moving mass. Hamed *et al.* (2019) studied bending behaviors of FG porous nanobeams with four types of porosity (i.e.; the classical power porosity function, the symmetric with mid-plane cosine function, bottom surface distribution and top surface distribution). Based on the high-order coupling (HOC) modeling theory, Li *et al.* (2019) investigated vibration control of a rotating rigid-flexible coupled smart FG beam structure with a lumped mass and two piezoelectric films in temperature field. Rajasekaran and Khaniki (2019) studied size-dependent forced vibration of non-uniform bi-directional FG beams embedded in elastic environment and carrying a moving harmonic mass. Wang *et al.* (2019) investigated vibration response of FG graphene nanoplatelet reinforced composite beam under two successive moving masses. Mohamed *et al.* (2019) and Emam *et al.* (2019) studied analytically postbuckling of imperfect nanobeam by using classical Euler beam theory. Hamed *et al.* (2020) and Eltahaer and Mohamed (2020) studied the buckling of sandwich composite beam under variable axial load with and without elastic foundation.

According to literature reviews, previous studies and authors' knowledge the transient dynamic response of two-dimensional beams with functionally graded layers under

different nonharmonic dynamic loads has not been investigated. So, this article tends to fill this gap and illustrates transient responses of sandwich FG deep beam under generalized force functions. The following paper is organized as follows: - Section 2 focused on problem formulation, which include kinematics assumptions of displacement fields, constitutive equations of 2D plane stress sandwich FG deep beams, force functions distribution in spatial and time domain, and derived equation of motion. The numerical procedures and discretization of the FG deep beam structure using finite element method and numerical Newmark implicit time integration is adopted in this section. Section 3 is devoted to validation and parametric studies to present effects of force type, gradation parameter, geometrical and dynamical parameters on the time response of deep multilayer FG beams. Main remarks and conclusion points are highlighted and summarized in Section 4.

2. Problem formulation

2.1 Mathematical formulation

A geometrical description of thick beam with five functionally graded layers under a dynamic point load $P(t)$ at midpoint is shown in Fig. 1. The beam has a length of L through the axial direction x -axis, and thickness h through the transverse z -axis. The functionally graded layers are located as symmetry according to mid-plane axis. The layers are perfectly bonded. The height of each layer is equal. Each layer has a gradation material property (i.e.; Young modulus E , Poisson's ratio ν , and density ρ) through transverse direction, those can be described by a power-law distribution as

$$E(z) = (E_T - E_B) \left[\frac{z}{h} + \frac{1}{2} \right]^n + E_B \quad (1a)$$

$$\nu(z) = (\nu_T - \nu_B) \left[\frac{z}{h} + \frac{1}{2} \right]^n + \nu_B \quad (1b)$$

$$\rho(z) = (\rho_T - \rho_B) \left[\frac{z}{h} + \frac{1}{2} \right]^n + \rho_B \quad (1c)$$

in which n is the positive power exponent parameter and subscript T and B being the top and bottom properties of the layers.

Based on the continuum mechanics, the thick beam is described by plane stress problem. Therefore, the kinematic strain-displacement relations are described by

$$\begin{Bmatrix} \varepsilon_{xx} \\ \varepsilon_{zz} \\ \gamma_{xz} \end{Bmatrix} = \begin{bmatrix} \frac{\partial}{\partial x} & 0 \\ 0 & \frac{\partial}{\partial z} \\ \frac{\partial}{\partial z} & \frac{\partial}{\partial x} \end{bmatrix} \begin{Bmatrix} u \\ w \end{Bmatrix} \quad (2)$$

in which u , w are the displacements in x and z directions, respectively. ε_{xx} and ε_{zz} are the normal in-plane strains, and γ_{xz} is the shear in-plane strain. The constitutive stress-strain equation, in a case of FG layer, can be represented as

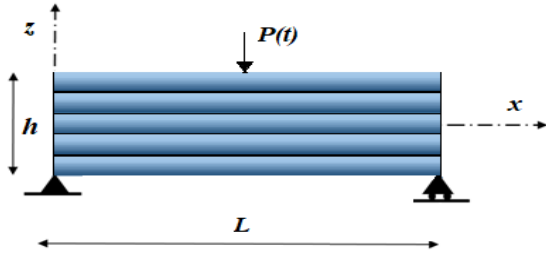


Fig. 1 Thick beam with five functionally graded layers under a dynamic point load

$$\begin{Bmatrix} \sigma_{xx} \\ \sigma_{zz} \\ \sigma_{xz} \end{Bmatrix} = \begin{bmatrix} C_{11}(z) & C_{12}(z) & 0 \\ C_{12}(z) & C_{22}(z) & 0 \\ 0 & 0 & C_{33}(z) \end{bmatrix} \begin{Bmatrix} \epsilon_{xx} \\ \epsilon_{zz} \\ \gamma_{xz} \end{Bmatrix} \quad (3)$$

where σ_{xx} , σ_{zz} are normal stresses, σ_{xz} is shear stress and coefficients of the stiffness can be described as functions of elasticity and Poisson's ratio as following:

$$C_{11}(z) = C_{22}(z) = \frac{E(z)}{1-\nu(z)^2}, \quad C_{33}(z) = \frac{E(z)}{2[1+\nu(z)]} \quad (4)$$

$$C_{12}(z) = \frac{\nu(z)E(z)}{1-\nu(z)^2}$$

Based on the virtual work, the dynamic equilibrium equation can be depicted as

$$\int_{\Omega} \delta \epsilon^T \sigma \, d\Omega - \int_{\Omega} \delta U^T [\mathbf{b} - \rho \ddot{\mathbf{U}}]^T \, d\Omega - \int_{\Gamma} \delta U^T P(t) \, d\Gamma = 0 \quad (5)$$

in which Ω is the occupied domain of the body, Γ is the boundary domain, \mathbf{b} is the body force per unit volume, and δU is the generalized virtual displacement. This equation can be represented in terms of displacement field and stiffness coefficients as following,

$$\int_A \left[C_{11}(z) \frac{\partial u}{\partial x} \frac{\partial \delta u}{\partial x} + C_{22}(z) \frac{\partial w}{\partial z} \frac{\partial \delta w}{\partial z} + C_{12}(z) \left[\frac{\partial u}{\partial z} + \frac{\partial w}{\partial x} \right] \left[\frac{\partial \delta u}{\partial z} + \frac{\partial \delta w}{\partial x} \right] + \rho(z) \ddot{u} \delta u + \rho(z) \ddot{w} \delta w \right] dA - \int_A t [b_x \delta u + b_z \delta w] dA - \int_{\Gamma} P(t) \delta w \, d\Gamma = 0 \quad (6)$$

where b_x and b_z are the body force components, \ddot{u} and \ddot{w} are the accelerations.

2.2 Finite element formulation

The considered problem is solved by using finite element method using the Twelve-node 2D-plane element model as illustrated in Fig. 2.

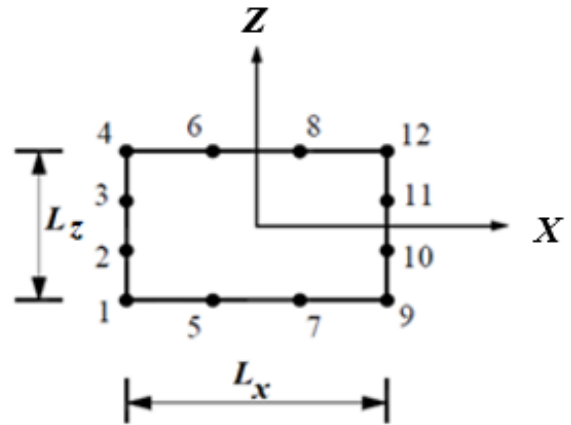


Fig. 2 Twelve-node 2D plane element

where L_x and L_y are element lengths in X and Z directions respectively. The displacement vector ($\{d\}$) for Twelve-node plane element is expressed as:

$$\{d\} = [\emptyset] \{d_n\} \quad \& \quad [\emptyset] = [\emptyset_1 \ \emptyset_2 \ \dots \ \emptyset_{12}] \quad (7)$$

where $\{d_n\}$ indicates the node displacement vector.

$$\{d_n\} = \begin{Bmatrix} u_1 \\ u_2 \\ \vdots \\ u_{12} \\ w_1 \\ w_2 \\ \vdots \\ w_{12} \end{Bmatrix} \quad (8)$$

where $\{d_n\}$ is the node displacement vector and its components are u_i and v_i are the displacement components for i node. The displacement of any generic element can be represented by its nodal values and corresponding functions as,

$$u = (u_1 \emptyset_1 + u_2 \emptyset_2 + u_3 \emptyset_3 + u_4 \emptyset_4 + u_5 \emptyset_5 + u_6 \emptyset_6 + u_7 \emptyset_7 + u_8 \emptyset_8 + u_9 \emptyset_9 + u_{10} \emptyset_{10} + u_{11} \emptyset_{11} + u_{12} \emptyset_{12}) \quad (9a)$$

$$w = (w_1 \emptyset_1 + w_2 \emptyset_2 + w_3 \emptyset_3 + w_4 \emptyset_4 + w_5 \emptyset_5 + w_6 \emptyset_6 + w_7 \emptyset_7 + w_8 \emptyset_8 + w_9 \emptyset_9 + w_{10} \emptyset_{10} + w_{11} \emptyset_{11} + w_{12} \emptyset_{12}) \quad (9b)$$

where \emptyset_i is the nonlinear interpolation shape functions, which can be represented as follows;

$$\emptyset_1 = \frac{1}{32} \left(1 - \frac{2X}{L_x} \right) \left(1 - \frac{2Z}{L_z} \right) \left(-10 + 9 \left(\frac{4X^2}{L_x^2} + \frac{4Z^2}{L_z^2} \right) \right),$$

$$\emptyset_2 = \frac{9}{32} \left(1 - \frac{2X}{L_x} \right) \left(1 - \frac{4Z^2}{L_z^2} \right) \left(1 - \frac{6Z}{L_z} \right) \quad (10)$$

$$\emptyset_3 = \frac{9}{32} \left(1 - \frac{2X}{L_x} \right) \left(1 - \frac{4Z^2}{L_z^2} \right) \left(1 + \frac{6Z}{L_z} \right),$$

$$\begin{aligned}\phi_4 &= \frac{1}{32} \left(1 - \frac{2X}{L_x}\right) \left(1 + \frac{2Z}{L_z}\right) \left(-10 + 9 \left(\frac{4X^2}{L_x^2} + \frac{4Z^2}{L_z^2}\right)\right) \\ \phi_5 &= \frac{9}{32} \left(1 - \frac{2Z}{L_z}\right) \left(1 - \frac{4X^2}{L_x^2}\right) \left(1 - \frac{6X}{L_x}\right), \\ \phi_6 &= \frac{9}{32} \left(1 + \frac{2Z}{L_z}\right) \left(1 - \frac{4X^2}{L_x^2}\right) \left(1 - \frac{6X}{L_x}\right) \\ \phi_7 &= \frac{9}{32} \left(1 - \frac{2Z}{L_z}\right) \left(1 - \frac{4X^2}{L_x^2}\right) \left(1 + \frac{6X}{L_x}\right), \\ \phi_8 &= \frac{9}{32} \left(1 + \frac{2Z}{L_z}\right) \left(1 - \frac{4X^2}{L_x^2}\right) \left(1 + \frac{6X}{L_x}\right) \\ \phi_9 &= \frac{1}{32} \left(1 + \frac{2X}{L_x}\right) \left(1 - \frac{2Z}{L_z}\right) \left(-10 + 9 \left(\frac{4X^2}{L_x^2} + \frac{4Z^2}{L_z^2}\right)\right), \\ \phi_{10} &= \frac{9}{32} \left(1 + \frac{2X}{L_x}\right) \left(1 - \frac{4Z^2}{L_z^2}\right) \left(1 - \frac{6Z}{L_z}\right) \\ \phi_{11} &= \frac{9}{32} \left(1 + \frac{2X}{L_x}\right) \left(1 - \frac{4Z^2}{L_z^2}\right) \left(1 + \frac{6Z}{L_z}\right), \\ \phi_{12} &= \frac{1}{32} \left(1 + \frac{2X}{L_x}\right) \left(1 + \frac{2Z}{L_z}\right) \left(-10 + 9 \left(\frac{4X^2}{L_x^2} + \frac{4Z^2}{L_z^2}\right)\right)\end{aligned}$$

Substituting equations (2), (7)-(10) into equation (6), the dynamic equilibrium equation is rewritten as follows: -

$$\begin{aligned}c \int_A \{\delta d_n\}^T ([B]^T [C] [B] \{d_n\} + \rho(Z) [\emptyset]^T [\emptyset] \{\delta \ddot{d}\}) dA \\ - \int_{\Gamma} \{\delta d_n\}^T [\emptyset]^T P(t) d\Gamma \\ - c \int_A \{\delta d_n\}^T [\emptyset]^T \begin{Bmatrix} b_x \\ b_z \end{Bmatrix} dA = 0\end{aligned} \quad (11)$$

where

$$[B] = \begin{bmatrix} \frac{\partial}{\partial X} & 0 \\ 0 & \frac{\partial}{\partial Y} \\ \frac{\partial}{\partial Y} & \frac{\partial}{\partial X} \end{bmatrix} [\emptyset], \quad [C] = \begin{bmatrix} C_{11}(z) & C_{12}(z) & 0 \\ C_{12}(z) & C_{22}(z) & 0 \\ 0 & 0 & C_{33}(z) \end{bmatrix} \quad (12)$$

After regulation of equation (11), the dynamic equilibrium equation written as follows:

$$[K] \{d_n\} + [M] \{\ddot{d}_n\} = \{F\} \quad (13)$$

where $[K]$, $[M]$, $\{F\}$ and $\{d_n\}$ are the stiffness matrix, mass matrix, load vector and displacement vector, respectively. The expansions of finite element matrices are represented as

$$[K] = c \int_A [B]^T [C] [B] dA \quad (14.a)$$

$$[M] = c \int_A \rho(z) [\emptyset]^T [\emptyset] dA \quad (14.b)$$

$$\{F\} = \int_{\Gamma} \{\delta d_n\}^T [\emptyset]^T P(t) d\Gamma + \quad (14.c)$$

$$c \int_A \{\delta d_n\}^T [\emptyset]^T \begin{Bmatrix} b_x \\ b_z \end{Bmatrix} dA$$

where, c is the width of the beam. The dynamic point load $P(t)$ is assumed to be sinusoidal harmonic, sinusoidal pulse or triangle in time domain as following

$$P(t) = P_0 \sin(\Omega t) \quad 0 \leq t \ll \infty \quad \text{Harmonic} \quad (15.a)$$

$$P(t) = P_0 \sin(\Omega t) \quad 0 \leq t \ll t_0 \quad \text{Sin Pulse} \quad (15.b)$$

$$P(t) = Pt \quad 0 \leq t \ll t_0 \quad \text{Triangle} \quad (15.c)$$

where, P_0 is the amplitude of the dynamic load and Ω is the frequency of the dynamic load. In the solution of eq. (13), implicit Newmark average acceleration ($\alpha=0.5$ & $\beta=0.25$) method is used in the time domain. In this procedure, the dynamic problem is transferred to system of static problem in each step as following

$$[\bar{K}(t, X)] \{d_n\}_{j+1} = \{\bar{F}(t)\} \quad (16)$$

in which

$$[\bar{K}(t, X)] = [K] + a_0 [M] \quad (17.a)$$

$$\{\bar{F}(t)\} = \{\bar{F}(t)\}_{j+1} + [M] \left(a_0 \{d_n\}_j + a_1 \{\dot{d}_n\}_j + a_2 \{\ddot{d}_n\}_j \right) \quad (17.b)$$

and constant coefficients can be evaluated by

$$a_0 = \frac{1}{\beta \Delta t^2}, \quad a_1 = \frac{1}{\beta \Delta t}, \quad a_2 = \frac{1-2\beta}{\beta} \quad (18)$$

After evaluating $\{d_n\}_{j+1}$ at a time $t_{j+1} = t_j + \Delta t$, the acceleration and velocity vectors can be evaluated by

$$\{\ddot{d}_n\}_{j+1} = a_0 (\{d_n\}_{j+1} - \{d_n\}_j) - a_1 \{\dot{d}_n\}_j - a_2 \{\ddot{d}_n\}_j \quad (19.a)$$

$$\{\dot{d}_n\}_{j+1} = \{\dot{d}_n\}_j + a_3 \{\ddot{d}_n\}_j + a_4 \{\ddot{d}_n\}_{j+1} \quad (19.b)$$

where $a_3 = (1 - \alpha)\Delta t$, and $a_4 = \alpha\Delta t$

3. Numerical results

In this section, effects of force type, gradation parameter, geometrical and stacking sequence of layers on the time response of thick multilayer FG beams. The materials of functionally graded layers are considered as Aluminum (Al; $E=70 \text{ GPa}$, $\nu=0.3$, $\rho=2702 \text{ kg/m}^3$) and Zirconia ($E=151 \text{ GPa}$, $\nu=0.3$, $\rho=3000 \text{ kg/m}^3$). The bottom surface of the FG layer is Zirconia, the top surface material of the FG layer is Aluminum. The dimensions of the FG thick beam are considered as follows: $c = 0.1 \text{ m}$, $h = 0.1 \text{ m}$ and the length of beam varied according to aspect ratio $L/h=3, 5, 10$ in the numerical process. The height of each layer is equal. The five-point Gauss rule is used for calculation of the integration.

In the numerical results, three different stacking sequences of layers are considered. The stacking sequences

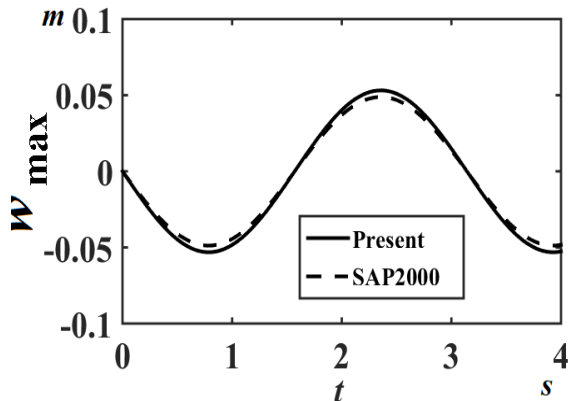


Fig. 3 Comparison study: Time responses of the fully Aluminium beam for $L/h=5$, $P_0=1000$ kN, $\Omega=2$ rad/s

of layers used are *stacking sequence 1*: five FGM layers, *stacking sequence 2*: FGM-Homogeneous-Homogeneous-FGM-FGM and *stacking sequence 3*: Homogeneous-Homogeneous-FGM-Homogeneous-Homogeneous layers.

3.1 Validation

To validate the current model, authors adopted previous model solved by Ritz procedure and In order to validate using method, a comparison study is performed. In the comparison study, the maximum vertical displacements of a fully Aluminum beam are obtained and compared with SAP2000 program for load 1 for $L/h=5$, $P_0=1000$ kN, $\Omega=2$ rad/s in figure 3. It is seen from figure 3, that results of this study are approximately identical with results of SAP2000.

3.2 Sinusoidal harmonic load

Through this section, a time response of FG thick beam structure under sinusoidal harmonic load with frequency $\Omega=2$ rad/s with 3 stacking sequences and different distribution parameters ($n=0, 0.5, 1$, and 2). The time responses for fully graded five layer sequences with different slenderness ratio is presented in figure 4. As shown in figure, the responses of three slenderness ratios have the same profile of applied force, identical time period, and with different deflection amplitudes. The maximum amplitude is observed in case of $L/h=10$ (note that, the amplitude of force in this case is one tenth of the amplitude of other cases), however, the minimum amplitude is noticed in case of $L/h=3$. Increasing L/h means a reduction in overall stiffness, which induces the more deflection amplitudes. It is observed at a specified slenderness ratio, the amplitude of deflection decreased by increasing the power exponent value n , because increasing the constituent of FG by zirconia that has higher elasticity rather than Aluminum that has lower elasticity.

All phenomena and notices observed in case of *stacking sequence 1* are observed in the other two cases *stacking sequences 2 and 3* as shown in figures 5 and 6, respectively. It is noticed in *stacking sequence 3*, the effect of graduation exponent n becomes insignificant and the deflection time

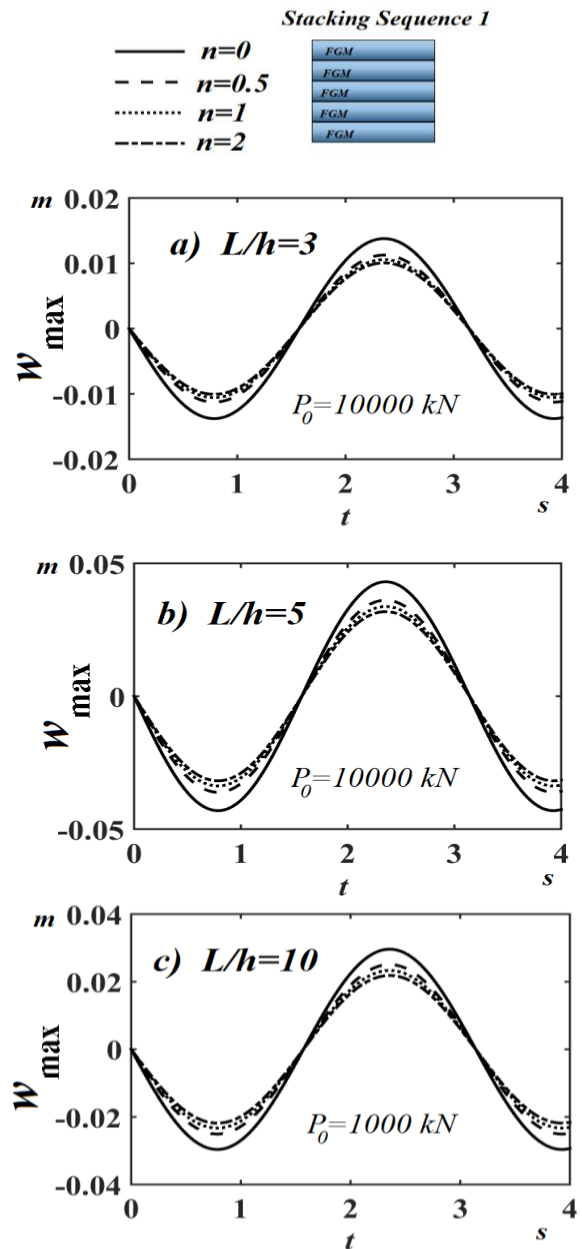


Fig. 4 Time responses of thick FG multilayer beam in *stacking sequence 1* with different n parameters for a) $L/h=3$, b) $L/h=5$ and c) $L/h=10$

response for any value of n is very identical with time response of isotropic thick beam. However, this *stacking sequence* structure may be effective in applications of thermal isolation. It is noted that, the stacking sequence has not any effect on the time period of oscillation, which means that the applied frequency is far from resonance frequency. This observation is consistent with the vibrational phenomenon of structures.

3.3 Sinusoidal pulse load

Deflection time responses for proposed three stacking sequences under dynamic sinusoidal pulse load with frequency $\Omega=2$ rad/s, are presented in figures (7-9). It is

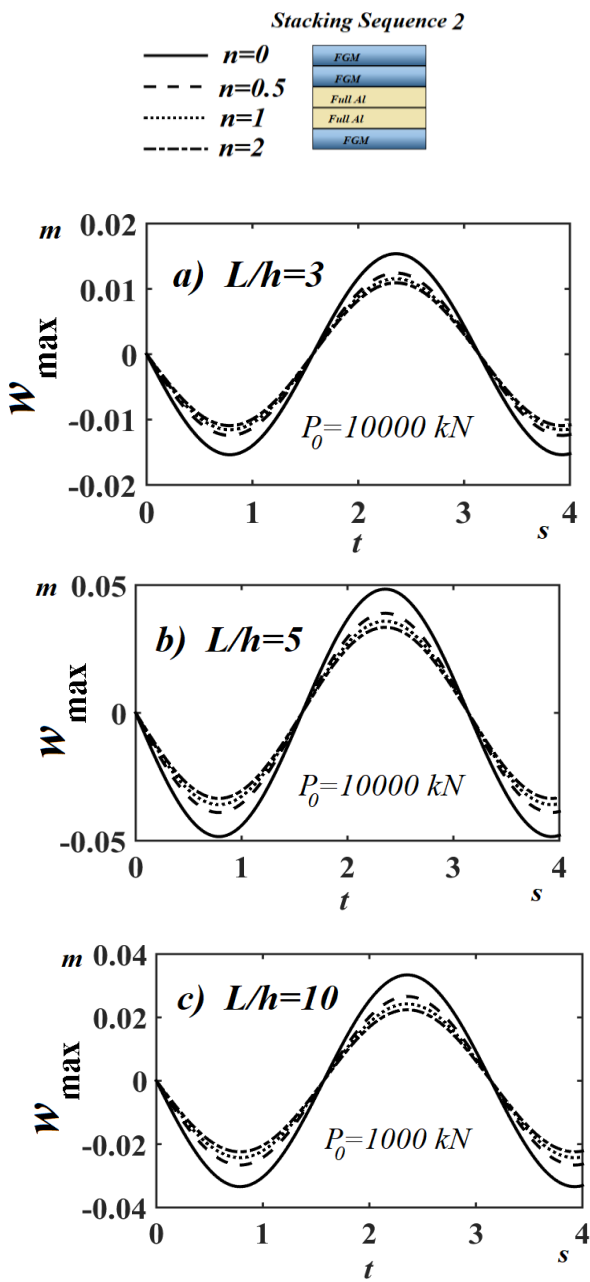


Fig. 5 Time responses of thick FG multilayer beam in stacking sequence 2 with different n parameters for a) $L/h=3$, b) $L/h=5$ and c) $L/h=10$

noted that, the deflection response follows the response of the force during time application. After removing load, the deflection reach to static equilibrium for smaller slenderness ratios at $L/h=3$ and 5. However, at $L/h=10$, small oscillation is observed after removing the load, and it is continuing for infinite.

For a specific stacking sequence and slenderness ratio, increasing the graduation parameter tends to decrease the overall amplitude of vibration, but it has not any effect on the time period of oscillations. It is noted that, the stacking sequence 1 is stiffer than stacking sequence 2, that is stiffer than stacking sequence 3. In case of hand, the graduation parameter is insignificant in stacking sequence 3.

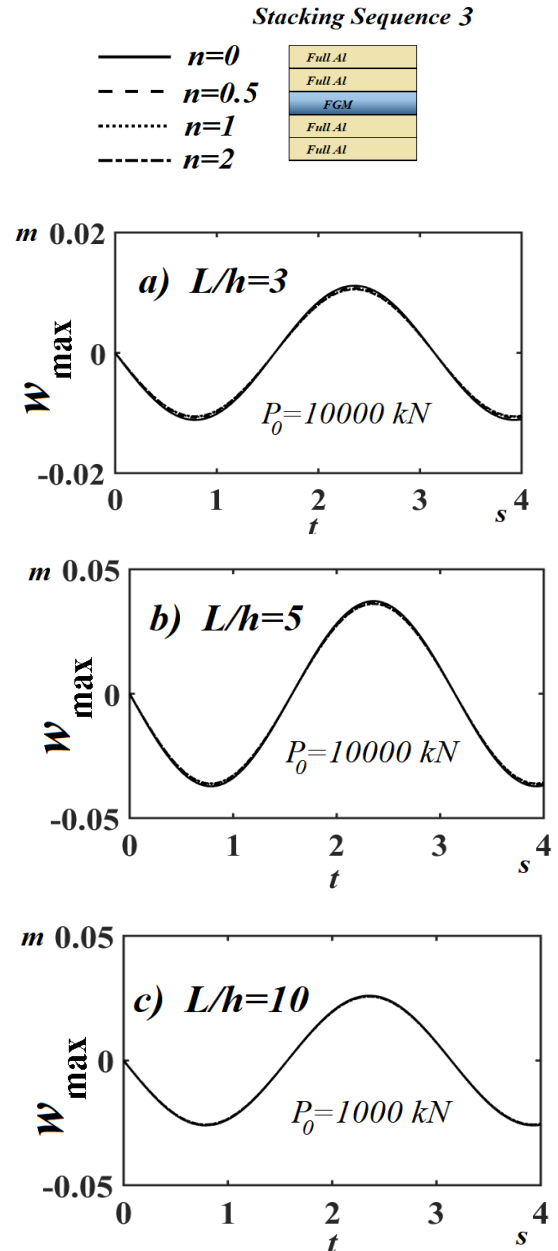


Fig. 6 Time responses of thick FG multilayer beam in stacking sequence 3 with different n parameters for a) $L/h=3$, b) $L/h=5$ and c) $L/h=10$

3.4 Triangle pulse load

The time responses of FG multilayer thick beam with varying stacking sequences under a triangle pulse load are presented in figures (10-12). As shown in figure 10 at $L/h=3$, the deflection time response of thick FG beam is increased linearly by increasing the load amplitude until 1 sec. After removing a load, the beam structure become stationary and return to its static equilibrium. It is noted, by increasing the graduation of Zirconia the deflection amplitude is decreased. As L/h increased from 3 to 5, small oscillation is appeared in steady state response. However, increasing the slenderness ratio from 5 to 10, significant oscillation is noticed and dominated for a steady state

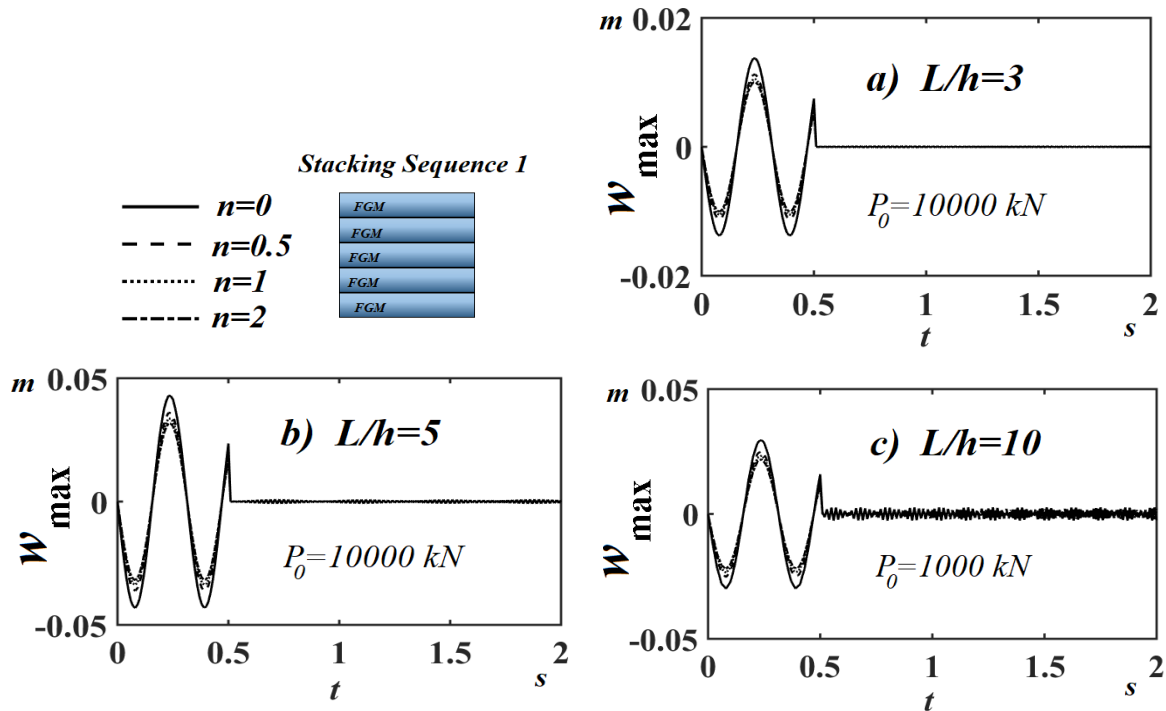


Fig. 7 Time responses of thick FG multilayer beam in stacking sequence 1 with different n parameters for a) $L/h=3$, a) $L/h=5$ and c) $L/h=10$

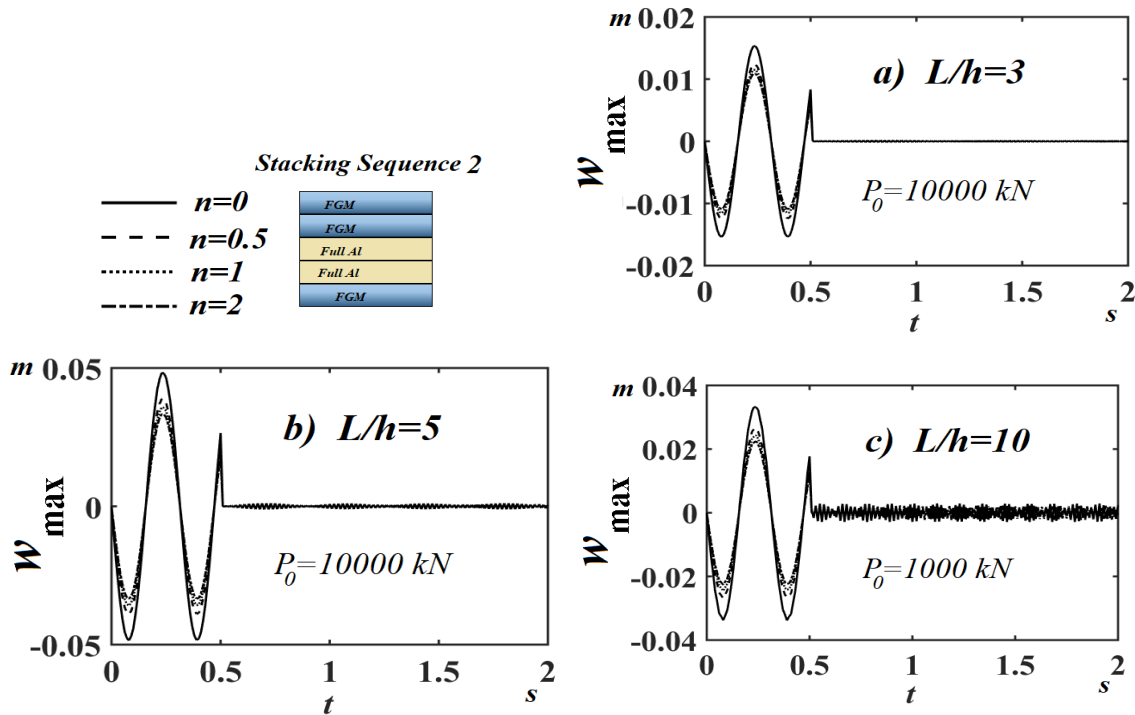


Fig. 8 Time responses of thick FG multilayer beam in stacking sequence 2 with different n parameters for a) $L/h=3$, a) $L/h=5$ and c) $L/h=10$

response after removing a load. All observations and phenomena noticed in stacking sequence 1 are dominated in other stacking sequences. In the other hand, changing the

stacking sequence 1 to stacking sequence 2, as shown in figure 11, the maximum deflection is increased because of a reduction in stiffness.

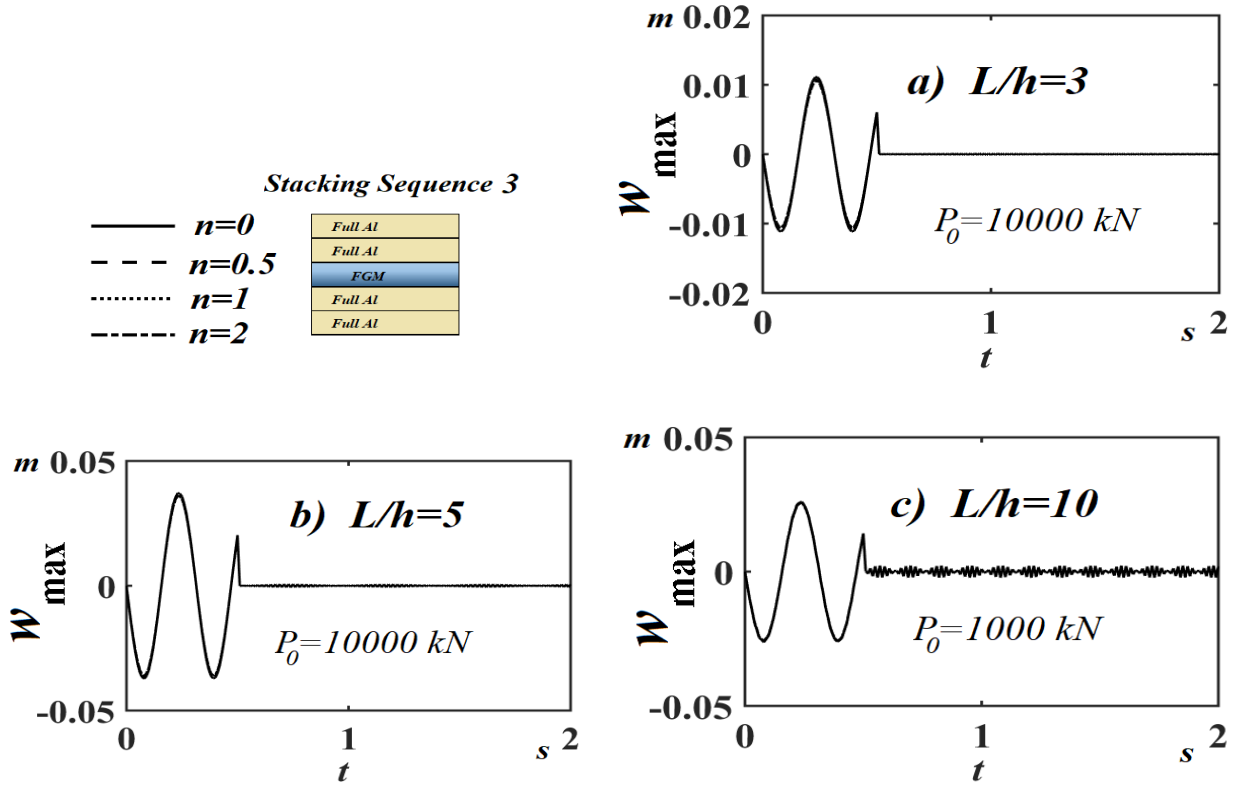


Fig. 9 Time responses of thick FG multilayer beam in stacking sequence 3 with different n parameters for a) $L/h=3$, a) $L/h=5$ and c) $L/h=10$

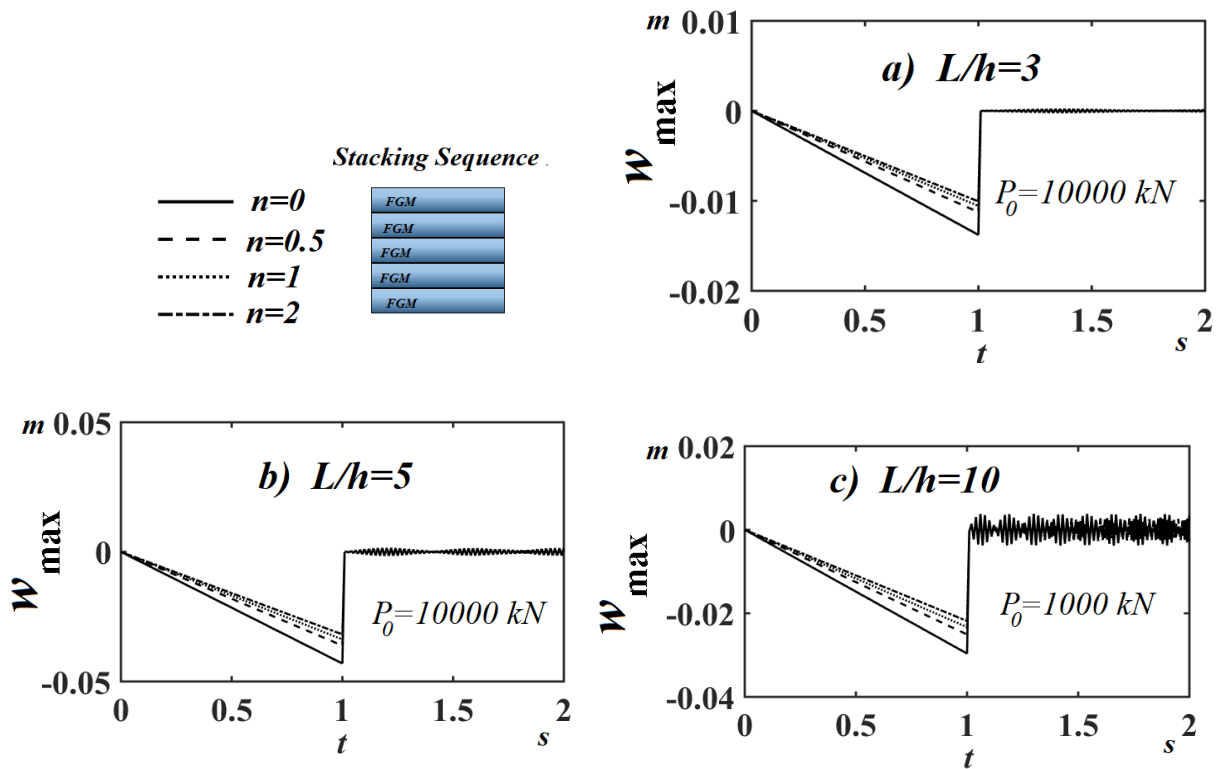


Fig. 10 Time responses of thick FG multilayer beam in stacking sequence 1 with different n parameters for a) $L/h=3$, a) $L/h=5$ and c) $L/h=10$

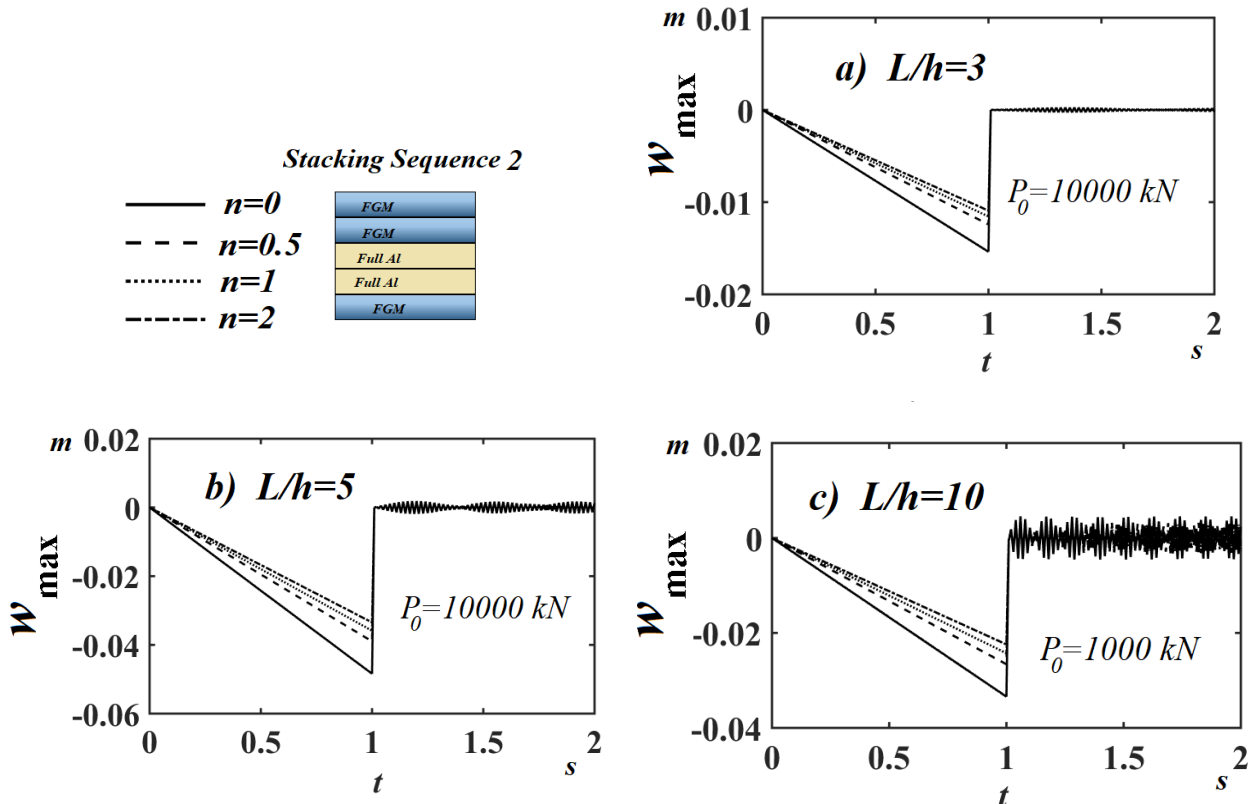


Fig. 11 Time responses of thick FG multilayer beam in stacking sequence 2 with different n parameters for a) $L/h=3$, a) $L/h=5$ and c) $L/h=10$.

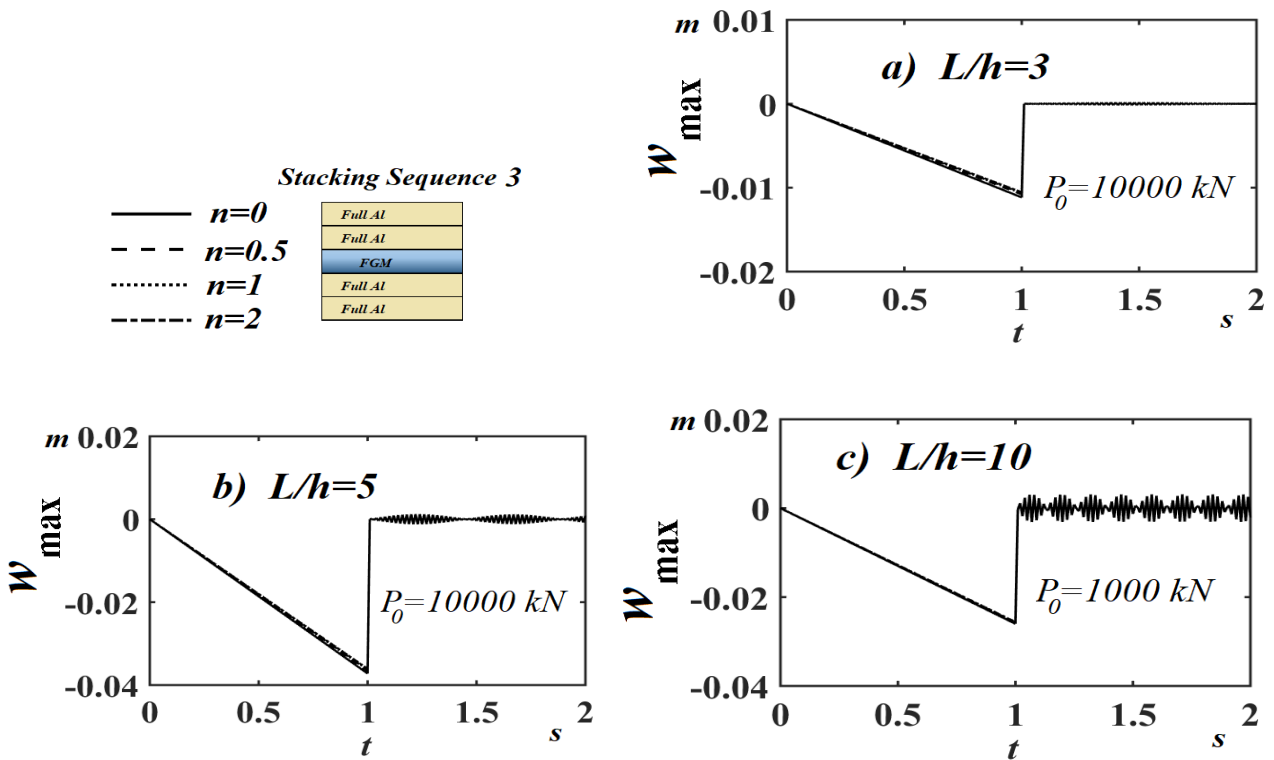


Fig. 12 Time responses of thick FG multilayer beam in stacking sequence 3 with different n parameters for a) $L/h=3$, a) $L/h=5$ and c) $L/h=10$.

4. Conclusions

The time response analyses of FG multilayer 2D deep beam with different stacking sequences under applied dynamic load have been investigated based on 2D plane stress constitutive equation. Three types of dynamic loads are exploited, which are sinusoidal harmonic, sinusoidal pulse or triangle in time. Finite element with Twelve-node 2D-plane element is exploited to discretize the beam domain and transferring the governing partial differential equation of motion to ordinary equation of motion. Newmark time integration is assumed to transform the dynamic problem to system of static problems at each time step. The comparison study shows the accuracy of proposed model. Several conclusions can be deduced from parametric studies as follows: -.

- The dynamic response of deep FG beam has the same profile as applied forces.
- Increasing slenderness ratio tends to increase the response amplitude and may generate steady state oscillation response at higher value at $L/h=10$.
- The graduation parameter has significant effect on the maximum deflection, especially for stacking sequences 1 and 2. However, in case of stacking sequence 3, the graduation parameter has not any effect on vibration amplitude.

Acknowledgments

This work was supported by the Deanship of Scientific Research (DSR), King Abdulaziz University, Jeddah, under Grant no. (DF-060-135-1441). The authors, therefore, gratefully acknowledge the DSR technical and financial support.

References

- Abdalrahmaan, A.A., Eltahaer, M.A., Kabeel, A.M., Abdraboh, A.M., and Hendi, A.A. (2019), "Free and Forced Analysis of Perforated Beams", *Steel Compos. Struct.*, **31**(5), 489-502. <https://doi.org/10.12989/scs.2019.31.5.489>.
- Akbaş, Ş.D. (2016), "Forced vibration analysis of viscoelastic nanobeams embedded in an elastic medium", *Smart Struct. Syst.*, **18**(6), 1125-1143. <http://dx.doi.org/10.12989/sss.2016.18.6.1125>
- Akbaş, Ş. D. (2017), "Forced vibration analysis of functionally graded nanobeams", *J. Appl. Mech.*, **9**(07), 1750100. <https://doi.org/10.1142/S1758825117501009>
- Akbaş, Ş. D. (2018a), "Forced vibration analysis of cracked nanobeams", *J. Brazilian Soc. Mech. Sci. Eng.*, **40**(8), 392. <https://doi.org/10.1007/s40430-018-1315-1>
- Akbaş, Ş. D. (2018b), "Forced vibration analysis of cracked functionally graded microbeams", *Adv. Nano Res.*, **6**(1), 39-55. <https://doi.org/10.12989/anr.2018.6.1.039>
- Akbaş, S. D. (2018c), "Investigation on Free and Forced Vibration of a Bi-Material Composite Beam", *Journal of Polytechnic-Politeknik Dergisi*, **21**(1), 65-73.
- Akbaş, Ş. D. (2019a), "Hygro-Thermal Nonlinear Analysis of a Functionally Graded Beam", *J. Appl. Comput. Mech.*, **5**(2), 477-485. <https://doi.org/10.22055/JACM.2018.26819.1360>
- Akbaş, Ş. D. (2019b), "Forced vibration analysis of functionally graded sandwich deep beams", *Coupl. Syst. Mech.*, **8**(3), 259-271. <https://doi.org/10.12989/csm.2019.8.3.259>
- Albino, J. C. R., Almeida, C. A., Menezes, I. F. M. and Paulino, G. H. (2018), "Co-rotational 3D beam element for nonlinear dynamic analysis of risers manufactured with functionally graded materials (FGMs)", *Eng. Struct.*, **173**, 283-299. <https://doi.org/10.1016/j.engstruct.2018.05.092>
- Almitani, K.H., Abdalrahmaan, A.A., Eltahaer, M.A., (2019), "On Forced and Free Vibrations of Cutout Squared Beams", *Steel Compos. Struct.*, **32**(5), 643-655. <https://doi.org/10.12989/scs.2019.32.5.643>
- Alshorbagy, A. E., Eltahaer, M. A. and Mahmoud, F. F. (2011), "Free vibration characteristics of a functionally graded beam by finite element method", *Appl. Math. Modell.*, **35**(1), 412-425. <https://doi.org/10.1016/j.apm.2010.07.006>
- Andrianov, I. V., Awrejcewicz, J. and Diskovsky, A. A. (2018), "Design optimization of FGM beam in stability problem", *Eng. Comput.*, **36**(1), 248-270. <https://doi.org/10.1108/EC-03-2018-0108>
- Assie, A. E., Eltahaer, M. A. and Mahmoud, F. F. (2011), "Behavior of a viscoelastic composite plates under transient load", *J. Mech. Sci. Technol.*, **25**(5), 1129. <https://doi.org/10.1007/s12206-011-0302-6>
- Attia, M. A., Eltahaer, M. A., Soliman, A., Abdelrahman, A. A. and Alshorbagy, A. E. (2018), "Thermoelastic Crack Analysis in Functionally Graded Pipelines Conveying Natural Gas by an FEM", *J. Appl. Mech.*, **10**(04), 1850036. <https://doi.org/10.1142/S1758825118500369>
- Chen, Y., Jin, G., Zhang, C., Ye, T. and Xue, Y. (2018), "Thermal vibration of FGM beams with general boundary conditions using a higher-order shear deformation theory", *Compos. Part B Eng.*, **153**, 376-386. <https://doi.org/10.1016/j.compositesb.2018.08.111>
- Doroushi, A., Eslami, M. R. and Komeili, A. (2011), "Vibration analysis and transient response of an FGPM beam under thermo-electro-mechanical loads using higher-order shear deformation theory", *J. Intelligent Mater. Syst. Struct.*, **22**(3), 231-243. <https://doi.org/10.1177/1045389X11398162>
- Eltahaer, M.A., Alshorbagy, A.E. and Mahmoud, F.F. (2013), "Determination of neutral axis position and its effect on natural frequencies of functionally graded macro/nanobeams", *Compos. Struct.*, **99**, 193-201. <https://doi.org/10.1016/j.compstruct.2012.11.039>
- Eltahaer, M. A., A. A. Abdelrahman, A. Al-Nabawy, M. Khater, and A. Mansour, (2014), "Vibration of nonlinear graduation of nano-Timoshenko beam considering the neutral axis position", *Appl. Math. Comput.*, **235**, 512-529. <https://doi.org/10.1016/j.amc.2014.03.028>
- Eltahaer, M. A., Attia, M. A., Soliman, A. E. and Alshorbagy, A. E. (2018a), "Analysis of crack occurs under unsteady pressure and temperature in a natural gas facility by applying FGM", *Struct. Eng. Mech.*, **66**(1), 97-111. <https://doi.org/10.12989/sem.2018.66.1.097>
- Eltahaer, M. A., Abdraboh, A. M. and Almitani, K. H. (2018b), "Resonance frequencies of size dependent perforated nonlocal nanobeam", *Microsyst. Technol.*, **24**(9), 3925-3937. <https://doi.org/10.1007/s00542-018-3910-6>
- Eltahaer, M. A., Mohamed, N., Mohamed, S. A. and Seddek, L. F. (2019a), "Periodic and nonperiodic modes of postbuckling and nonlinear vibration of beams attached to nonlinear foundations", *Appl. Math. Modell.*, **75**, 414-445. <https://doi.org/10.1016/j.apm.2019.05.026>
- Eltahaer, M. A., Omar, F. A., Abdalla, W. S. and Gad, E. H. (2019b), "Bending and vibrational behaviors of piezoelectric nonlocal nanobeam including surface elasticity", *Waves in Random and Complex Media*, **29**(2), 264-280. <https://doi.org/10.1080/17455030.2018.1429693>
- Eltahaer, M.A., Mohamed, S.A., (2020), "Buckling and Stability Analysis of Sandwich Beams subjected to Varying Axial Loads", *Steel Compos. Struct.*, **34**(2), 241-260.

- <https://doi.org/10.12989/scs.2020.34.2.241>
- Emam, S., Eltaher, M., Khater, M. and Abdalla, W. (2018), "Postbuckling and Free Vibration of Multilayer Imperfect Nanobeams under a Pre-Stress Load", *Appl. Sci.*, **8**(11), 2238. <https://doi.org/10.3390/app8112238>
- Esen, I. (2019), "Dynamic response of a functionally graded Timoshenko beam on two-parameter elastic foundations due to a variable velocity moving mass", *J. Mech. Sci.*, **153**, 21-35. <https://doi.org/10.1016/j.ijmecsci.2019.01.033>
- Hamed, M. A., Sadoun, A. M. and Eltaher, M.A. (2019), "Effects of porosity models on static behavior of size dependent functionally graded beam", *Struct. Eng. Mech.*, **71**(1), 89-98. <https://doi.org/10.12989/sem.2019.71.1.089>
- Hamed M.A., Mohamed, S.A., Eltaher, M.A., (2020), "Buckling Analysis of Sandwich Beam Rested on Elastic Foundation and Subjected to Varying Axial In-Plane Loads", *Steel Compos. Struct.*, **34**(1), 75-89. <https://doi.org/10.12989/scs.2020.34.1.075>
- He, X. Q., Ng, T. Y., Sivashanker, S. and Liew, K. M. (2001), "Active control of FGM plates with integrated piezoelectric sensors and actuators", *J. Solids Struct.*, **38**(9), 1641-1655. [https://doi.org/10.1016/S0020-7683\(00\)00050-0](https://doi.org/10.1016/S0020-7683(00)00050-0)
- Huang, Y., Wang, T., Zhao, Y. and Wang, P. (2018), "Effect of axially functionally graded material on whirling frequencies and critical speeds of a spinning Timoshenko beam", *Compos. Struct.*, **192**, 355-367. <https://doi.org/10.1016/j.compstruct.2018.02.039>
- Li, L., Liao, W. H., Zhang, D. and Zhang, Y. (2019), "Vibration control and analysis of a rotating flexible FGM beam with a lumped mass in temperature field", *Compos. Struct.*, **208**, 244-260. <https://doi.org/10.1016/j.compstruct.2018.09.070>
- Malekzadeh, P. and Monajjemzadeh, S.M. (2013), "Dynamic response of functionally graded plates in thermal environment under moving load", *Compos. Part B Eng.*, **45**(1), 1521-1533. <https://doi.org/10.1016/j.compositesb.2012.09.022>
- Malekzadeh, P. and Monajjemzadeh, S. M. (2015), "Nonlinear response of functionally graded plates under moving load", *Thin-Wall. Struct.*, **96**, 120-129. <https://doi.org/10.1016/j.tws.2015.07.017>
- Mohamed, N., Eltaher, M.A., Mohamed, S. and Seddek, L.F. (2019), "Energy Equivalent Model in Analysis of Postbuckling of Imperfect Carbon Nanotubes Resting on Nonlinear Elastic Foundation", *Struct. Eng. Mech.*, **70**(6), 737-750. <https://doi.org/10.12989/sem.2019.70.6.737>
- Rajasekaran, S. and Khaniki, H. B. (2019), "Size-dependent forced vibration of non-uniform bi-directional functionally graded beams embedded in variable elastic environment carrying a moving harmonic mass", *Appl. Math. Modell.*, **72**, 129-154. <https://doi.org/10.1016/j.apm.2019.03.021>
- Shoostari, A. and Raffie, M. (2011), "Nonlinear forced vibration analysis of clamped functionally graded beams", *Acta Mechanica*, **221**(1-2), 23. <https://doi.org/10.1007/s00707-011-0491-1>
- Şimşek, M. and Kocatürk, T. (2009), "Free and forced vibration of a functionally graded beam subjected to a concentrated moving harmonic load", *Compos. Struct.*, **90**(4), 465-473. <https://doi.org/10.1016/j.compstruct.2009.04.024>
- Şimşek, M. (2010), "Vibration analysis of a functionally graded beam under a moving mass by using different beam theories", *Compos. Struct.*, **92**(4), 904-917. <https://doi.org/10.1016/j.compstruct.2009.09.030>
- Su, Z., Jin, G. and Ye, T. (2016), "Vibration analysis and transient response of a functionally graded piezoelectric curved beam with general boundary conditions", *Smart Mater. Struct.*, **25**(6), 065003. <https://doi.org/10.1088/0964-1726/25/6/065003>
- Wang, Y. and Wu, D. (2016), "Thermal effect on the dynamic response of axially functionally graded beam subjected to a moving harmonic load", *Acta Astronautica*, **127**, 171-181. <https://doi.org/10.1016/j.actaastro.2016.05.030>
- Wang, Y., Xie, K., Fu, T. and Shi, C. (2019), "Vibration response of a functionally graded graphene nanoplatelet reinforced composite beam under two successive moving masses", *Compos. Struct.*, **209**, 928-939. <https://doi.org/10.1016/j.compstruct.2018.11.014>
- Xiang, H. J. and Yang, J. (2008), "Free and forced vibration of a laminated FGM Timoshenko beam of variable thickness under heat conduction", *Compos. Part B Eng.*, **39**(2), 292-303. <https://doi.org/10.1016/j.compositesb.2007.01.005>
- Yang, J., Chen, Y., Xiang, Y. and Jia, X. L. (2008), "Free and forced vibration of cracked inhomogeneous beams under an axial force and a moving load", *J. Sound Vib.*, **312**(1-2), 166-181. <https://doi.org/10.1016/j.jsv.2007.10.034>

CC